Mixed-Valent Compounds

DOI: 10.1002/anie.201006695

Two Linear Undecanickel Mixed-Valence Complexes: Increasing the Size and the Scope of the Electronic Properties of Nickel Metal Strings**

Rayyat H. Ismayilov, Wen-Zhen Wang, Gene-Hsiang Lee, Chen-Yu Yeh, Shao-An Hua, You Song, Marie-Madeleine Rohmer†, Marc Bénard, and Shie-Ming Peng**

In memory of Marie-Madeleine Rohmer

The importance of one-dimensional (1D) transition-metal complexes stems from their ability to provide a fundamental understanding of metal–metal interactions and electron transport along an extended metal-atom chain (EMAC),[1] and from the perspective of taking advantage of their specific properties for potential applications, such as molecular metal wires and switches.[2] A series of string complexes of oligo-α-pyridylamino ligands ranging from 3 to 9 core metal atoms has been synthesized and characterized by Cotton's group and our group.[3] Attempts to characterize such very long EMACs with high electron conductivity were hindered by the synthetic difficulties rapidly increasing with the size of the metal chain. We synthesized $[Ni_9(\mu_9\text{-peptea})_4Cl_2]$ ten years ago,[4] but all attempts to characterize a longer chain of Ni atoms have, to date, been unsuccessful, owing to very low yields and to the instability of the target compound, probably because of the high flexibility of large pyridylamino ligands.

Recently we developed a new family of ligands by substituting rigid and potentially redox active naphthyridine (na) groups for the pyridine (py) rings. Naphthyridine-modulated ligands stabilize nickel ions in a low oxidation state, giving rise to mixed-valent $[Ni_2(napy)_4]^{3+}$ units (napy = naphthyridine).[5] Using this strategy,[6] we obtained a series of stable, low-oxidation-state-nickel string complexes combining mixed-valency, a property important in the development of novel electronic materials,[7] with an enhanced electron mobility, which is able to increase the conductance of molecular metal wires.[8]

We report a new tetranaphthyridyltriamine ligand, N^2-(2-(1,8-naphthyridin-7-ylamino)-1,8-naphthyridin-7-yl)-N^7-(1,8-naphthy-ridin-2-yl)-1,8-naphthyridine-2,7-diamine (H_3tentra) and two undecanickel complexes of the deprotonated tentra trianion, $[Ni_{11}(tentra)_4Cl_2](PF_6)_4$ (**1**) and $[Ni_{11}(tentra)_4(NCS)_2](PF_6)_4$ (**2**).

The ligand H_3tentra was synthesized on the basis of Buchwald's palladium-catalyzed procedures by the cross-coupling of bis(2-chloro-1,8-naphthyridin-7-yl)amine and 2-amino-1,8-naphthyridine. Undecametallic complex $[Ni_{11}(tentra)_4Cl_2](PF_6)_4$ (**1**) was obtained by the reaction of anhydrous $NiCl_2$ with the H_3tentra ligand in an argon atmosphere employing naphthalene as solvent and *t*BuOK as a base to deprotonate the amine groups. The thiocyanate species (**2**) was obtained from **1** by an axial ligand exchange reaction.

The crystal structures of **1** and **2** are shown in Figure 1 and the Supporting Information Figure 1S, respectively. Both **1** and **2** are tetracationic molecules associated each with four PF_6^- counterions. They crystallize in unusually large cells, with one dimension exceeding 50 Å. The Ni_{11} chain of **1** and **2** is linear and wrapped in a helical manner by four tentra trianions. In both complexes, the atoms of the axial ligands are collinear with the Ni_{11} axis; the molecular lengths are 27.7 and 32.4 Å for **1** and **2**, respectively. These are the longest EMAC complexes reported to date. The nature of the axial ligand does not significantly affect the metal–metal bond length, and no obvious structural change is observed for compound **2** with respect to **1**. Therefore, we will only analyze the structure of **1** in detail. Selected bond lengths for **1** are displayed in Figure 1c together with the corresponding values obtained from geometry optimization at the DFT/B3LYP level.

Molecule **1** consists of eleven nickel atoms in a linear chain with the Ni-Ni-Ni bond angles in the range of 179–180°. The N-Ni-Ni-N torsion angles for adjacent nickel are between 13.0 and 18.7°, much smaller than those in oligo-α-pyridylamino ligand EMAC complexes (ca. 22.5°).[4] Metal–metal distances usually decrease from the end to the center of the chain in both nickel and cobalt EMACs of oligo-α-pyridyl-

[*] Dr. R. H. Ismayilov, Dr. W.-Z. Wang, Dr. G.-H. Lee, S.-A. Hua, Prof. Dr. S.-M. Peng
Department of Chemistry, National Taiwan University
1, Sec. 4, Roosevelt Road, Taipei, 106 (Taiwan, ROC)
Fax: (+886) 2-8369-3765
E-mail: smpeng@ntu.edu.tw
Prof. Dr. C.-Y. Yeh
Department of Chemistry, National Chung Hsing University
Taichung (Taiwan, ROC)
Prof. Dr. Y. Song
Coordination Chemistry Institute and the State Key Laboratory of Coordination Chemistry Nanjing University, Nanjing 210093 (PRC)
Dr. M.-M. Rohmer, Dr. M. Bénard
Laboratoire de Chimie Quantique, Institut de Chimie
UMR 7177, 4, rue Blaise Pascal, 67000 Strasbourg (France)
Fax: (+33) 390-241-301
E-mail: benard@chimie.u-strasbg.fr

[†] Deceased.

[**] We thank the National Science Council and Ministry of Education of Taiwan, as well as the CNRS and the Ministère de l'Enseignement Supérieur et de la Recherche (France) for financial support.

Supporting information for this article is available on the WWW under http://dx.doi.org/10.1002/anie.201006695.

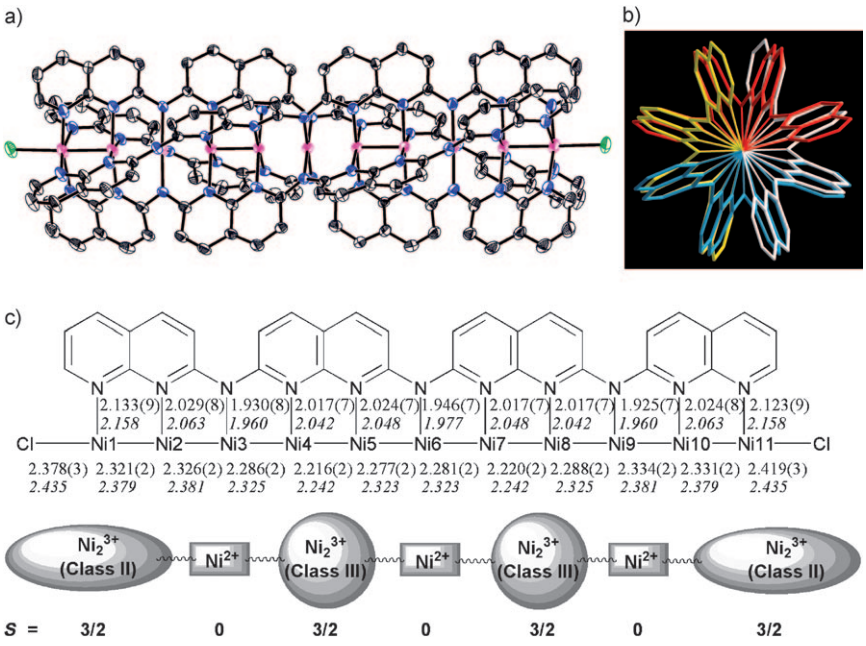

Figure 1. a) The ORTEP of $[Ni_{11}(tentra)_4Cl_2]^{4+}$. Thermal ellipsoids are set at 30% probability. The hydrogen atoms are omitted for clarity (Ni pink, N blue, Cl green, C black). b) View illustrating the quadruple helix along the metal-chain axis. c) Top: Selected interatomic distances observed and computed (B3LYP calculations, italic) for **1**. Bottom: The proposed valence and spin-state representation for nickel atoms in **1** and **2** (see text for details).

amido ligand.[3a,c] However, this regular change of the metal–metal distances along the chain is counteracted in **1** and **2** by the tendency of Ni–Ni distances to shorten when the nickel centers are bonded to naphthyridyl units. Accordingly, terminal Ni1–Ni2 distances are slightly shorter than the next Ni2–Ni3 distances, whereas the other naphthyridyl-bridged Ni4–Ni5 distance is significantly shorter than the innermost metal–metal contact, Ni5–Ni6. These trends are well reproduced by DFT calculations and might result from partial metal–metal bonds between the nickel atoms bonded to naphthyridyl units, promoted by the rigidity of the bicyclic structure. All Ni–N_{naph} bond lengths (2.017(7)–2.133(9) Å) are longer than those of Ni–N_{amido} (1.925(7)–1.946(7) Å), suggesting the occupancy of an antibonding orbital by the extra electrons. In agreement with DFT calculations, the charge distribution in the metal chain of **1** can therefore be described as Ni_2^{3+}-Ni^{2+}-Ni_2^{3+}-Ni^{2+}-Ni_2^{3+}-Ni^{2+}-Ni_2^{3+}, in which Ni_2^{3+} represents a mixed-valence $[Ni_2(napy)_4]^{3+}$ unit (Figure 1c).

The nature of Ni_2^{3+} units was previously investigated experimentally and theoretically by Bencini et al. and also recently in our group.[5d,6b] It is interesting that the two types of Ni_2^{3+} units involved in **1** or **2** behave somewhat differently. On the one hand, in Ni_2^{3+} units occupying terminal positions (Ni1–Ni2 and Ni10–Ni11) the metal atoms are in different environments: the coordination of Ni1 and Ni11 is square pyramidal instead of the square planar found for the neighboring metal, and these two outermost Ni atoms are more loosely attached to the equatorial nitrogen atoms than their neighbor in the metal chain. Since complete electron delocalization can be effective only in symmetric structures,[5d] the asymmetric outermost Ni_2^{3+} units are expected to belong to the Class II of the Robin–Day classification,[9] namely, mixed-valence species with a relatively weak electronic interaction between the sites. As proposed in a previous study,[8] the extra electron was initially accommodated in the $d_{x^2-y^2}$ orbital of square-planar nickel centers Ni2 or Ni10. This reduction step induced a partial transfer to the d_{z^2} orbital of pyramidal nickel centers Ni1 or Ni11 through the σ antibonding fragment orbital, leading to a spin state $S = 3/2$ for the Ni_2^{3+} unit.[8]

On the other hand, the analysis on the X-ray crystal structures of **1** and **2** confirm that in the inner mixed-valence units (Ni4–Ni5 and Ni7–Ni8), both metals are in identical environments and therefore should retain an equal share of the unpaired electrons. Therefore, the inner $[Ni_2(napy)_4]^{3+}$ units should be assigned to Class III (electron-delocalized) of the Robin–Day classification.[9] The results of DFT calculations and magnetic measurements are indeed consistent with a spin state $S = 3/2$ for the inner mixed-valent dinickel units Ni_2^{3+}. Mulliken atomic spin populations calculated for the high-spin state of **1** are +1.32 e and +1.27 e for Ni4 and Ni5, respectively, emphasizing the symmetry of the innermost $[Ni_2(napy)_4]^{3+}$ units and the almost complete delocalization of the spin density over the two metal atoms of these units. The spin populations for Ni1 and Ni2 are +1.48 e and +1.15 e, respectively, illustrating a somewhat larger asymmetry of the external $[Ni_2(napy)_4]^{3+}$ units (Supporting Information, Table 1S).

The nickel atoms bonded to amino nitrogen atoms display a square-planar coordination and the short Ni–N_{amido} bond (e.g. in **1**, 1.930(8), 1.946(7), and 1.925(7) Å for Ni3–N, Ni6–N, and Ni9–N, respectively) are indicative of Ni^{2+} atoms in a low-spin ($S = 0$) state. In the context of mixed valency, such fully localized metal sites should be assigned to Class I of the Robin—Day classification. The terminal Ni–N_{naph} bonds are the longest (2.133(9) and 2.123(9) Å for Ni1–N and Ni11–N, respectively) of all the Ni–N_{naph} bonds (2.017(7)–2.133(9) Å) and are consistent with the formation of mixed-valence dinickel units (Ni_2^{3+}) with a spin state $S = 3/2$.[8]

The redox properties of EMACs are an important topic in the research of metal–metal bonding and their potential application as molecular devices. The cyclic voltammograms of **1** and **2** were measured in the range −1.2 to +0.4 V, and showed five reversible, one-electron redox couples at $E_{1/2} =$ +0.27, +0.10, −0.31, −0.65, and −0.85 V for **1**, and at $E_{1/2} =$ +0.34, +0.19, −0.27, −0.58, and −0.82 V for **2** (Figure 2 and Supporting Information Figure 2S). In both complexes, all the electrochemical processes slightly overlap but can be well resolved by using differential pulse techniques. Both **1** and **2** are unstable beyond +0.4 V. The change from chlorides (**1**) to thiocyanates (**2**) results in slightly anodic shifts. The redox

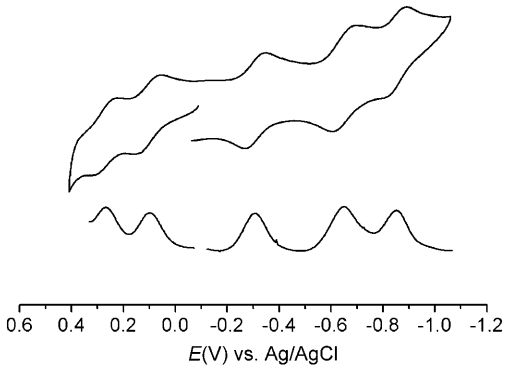

Figure 2. The cyclic voltammogram and differential pulse voltammogram of **1** in CH_2Cl_2 with 0.1 M tetrabutyl ammonium perchlorate (TBAP).

couple at $E_{1/2} = +0.10$ V in **1** is assigned to the electrochemical process $[Ni_{11}(tentra)_4Cl_2]^{4+}/[Ni_{11}(tentra)_4Cl_2]^{3+}$ as evidenced by thin-layer spectroelectrochemical measurements (Supporting Information Figure S3).

The near-IR spectra of **1** and **2** were recorded from 6000 to 11000 cm^{-1} in CH_3CN solution (Figure 3 and Supporting Information Figure S4). Each mixed-valence complex shows a

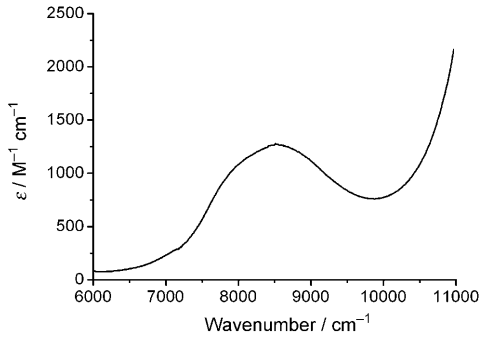

Figure 3. Near-IR spectrum of complex **1** in CH_3CN.

broad absorption band centered at 8377 cm^{-1} ($\varepsilon = 1636\,M^{-1}cm^{-1}$) for **1** and at 8525 cm^{-1} ($\varepsilon = 1271\,M^{-1}cm^{-1}$) with a shoulder at 7925 cm^{-1} ($\varepsilon = 1031\,M^{-1}cm^{-1}$) for **2**. These band systems are characteristic of intervalence charge-transfer transitions (IVCT).[10] Compared to pentanickel species $[Ni_5(bna)_4Cl_2](PF_6)_2$, these IVCT bands suggest a stronger electron coupling between the metal atoms in **1** and **2**.[8]

The magnetic susceptibility of **1** and **2** was measured over a temperature range of 2–300 K (Figure 4 and Supporting Information Figure S5). Both exhibit similar magnetic properties. Studies on oligopyridylamido nickel(II) EMACs established that the terminal Ni atoms display the spin state $S = 1$ associated with square-pyramidal coordination geometry, whereas the inner nickel centers are diamagnetic in accord with a square-planar coordination.[3c,11] The case of **1** and **2** appears different, however, since all four extra electrons distributed over the reduced Ni_2^{3+} units also contribute to magnetic moments. The results of crystal-structure analysis and DFT calculations are consistent with a spin state of $S =$

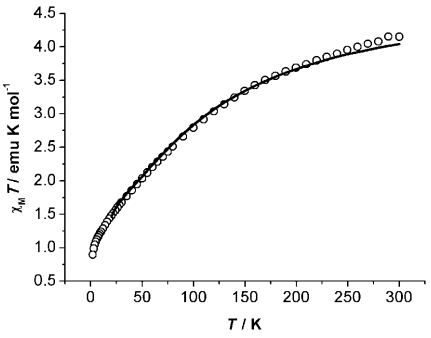

Figure 4. Plots of $\chi_M T$ versus T for compound **1**. The solid line represents the best theoretical fit.

3/2 for both the terminal and the inner mixed-valence Ni_2^{3+} units, while all nickel atoms coordinated to amido nitrogen are diamagnetic ($S = 0$). Thus the magnetic contribution could be assigned to a tetranuclear system $\boldsymbol{S} = \boldsymbol{S}_1 + \boldsymbol{S}_2 + \boldsymbol{S}_3 + \boldsymbol{S}_4$ in which $\boldsymbol{S}_1$, $\boldsymbol{S}_2$, $\boldsymbol{S}_3$, and $\boldsymbol{S}_4$ represent the local spins of Ni_2^{3+} units with $\boldsymbol{S}_1 = \boldsymbol{S}_2 = \boldsymbol{S}_3 = \boldsymbol{S}_4 = 3/2$ (Figure 1c). The $\chi_M T$ values at 300 K (4.15 and 4.49 emu K mol^{-1} for **1** and **2**, respectively) are significantly lower than the theoretical spin-only value (7.50 emu $K\,mol^{-1}$), because of the relatively strong antiferromagnetic interaction. Therefore, the tetranuclear model with a Hamiltonian $\boldsymbol{H} = -2J_{12}\boldsymbol{S}_1\boldsymbol{S}_2 - 2J_{23}\boldsymbol{S}_2\boldsymbol{S}_3 - 2J_{34}\boldsymbol{S}_3\boldsymbol{S}_4$, where each Ni_2^{3+} unit is considered as a single magnetic center, is used for fitting the $\chi_M T$ curve of complex **1**. Calculations were performed with the MAGPACK package.[12] The best fit above 30 K corresponds to: $g = 2.09$, $J_{12} = J_{34} = -40.83$ cm^{-1}, $J_{23} = -58.26$ cm^{-1}, indicative of relatively strong antiferromagnetic couplings between mixed-valence Ni_2^{3+} units. Broken-symmetry (BS) calculations carried out at the DFT/B3LYP level confirm the existence of a global antiferromagnetic interaction among the four Ni_2^{3+} units, since the state of lowest energy was identified as a singlet BS state ($S = 0$), associated with an energy 60 cm^{-1} below that of the reference high-spin state ($S = 6$) in which all spins are oriented in parallel (see Supporting Information).

To summarize, the linear undecanickel complexes $[Ni_{11}(tentra)_4Cl_2](PF_6)_4$ (**1**) and $[Ni_{11}(tentra)_4(NCS)_2](PF_6)_4$ (**2**) were synthesized using the tetranaphthyridyltriamine (H_3tentra) ligand, and structurally characterized. Compounds **1** and **2** are four-electron reduced species whose metal core can be described, according to crystallographic analysis and DFT calculations, as a series of four mixed-valence $[Ni_2(napy)_4]^{3+}$ units each separated by a square-planar Ni^{2+} unit, in the sequence Ni_2^{3+}-Ni^{2+}-Ni_2^{3+}-Ni^{2+}-Ni_2^{3+}-Ni^{2+}-Ni_2^{3+}. They are the longest finite metal-atom chains obtained to date. Temperature-dependent magnetic susceptibility curves are consistent with a system of four magnetic centers with $S = 3/2$, 3/2, 3/2, 3/2, each associated with a Ni_2^{3+} unit which is considered as a single center. Relatively strong antiferromagnetic couplings between mixed-valence Ni_2^{3+} units above 30 K were fitted for **1** by the set of parameters $g = 2.09$, $J_{12} = J_{34} = -40.83$ cm^{-1} and $J_{23} = -58.26$ cm^{-1}. It should finally be noted that **1** and **2** are the first examples of metal string complexes gathering within a single molecule all three classes of the Robin–Day classification of mixed valency.

Experimental Section

Synthesis: Full experimental details and analytical data can be found in the Supporting information.

Crystal data for **1**: $C_{160}H_{159}Cl_2F_{24}N_{45}Ni_{11}O_{12}P_4$, $M_r = 4200.91$, monoclinic, space group $P21/n$, $a = 13.5264(3)$, $b = 53.9494(11)$, $c = 25.4997(5)$ Å, $\beta = 100.7328°$, $V = 18282.7(7)$ Å^3, $Z = 4$, $\rho_{calcd} = 1.526$ mg m^{-3}, $R_1 = 0.0928$, $wR_2 = 0.2676$.

Crystal data for **2**: $C_{144}H_{100}Cl_{28}F_{24}N_{46}Ni_{11}P_4S_2$, $M_r = 4757.11$, monoclinic, space group $C2/c$, $a = 21.453(2)$, $b = 14.6068(13)$, $c = 55.4997(5)$ Å, $\beta = 94.452°$, $V = 17375(3)$ Å^3, $Z = 4$, $\rho_{calcd} = 1.819$ mg m^{-3}, $R_1 = 0.0980$, $wR_2 = 0.2745$.

Details on data collection are given in the Supporting information. CCDC 796456 (**1**) and 796457 (**2**) contain the supplementary crystallographic data for this paper. These data can be obtained free of charge from The Cambridge Crystallographic Data Centre via www.ccdc.cam.ac.uk/data_request/cif.

Received: October 25, 2010
Revised: December 13, 2010
Published online: February 11, 2011

Keywords: electronic structure · magnetic properties · metal–metal interactions · mixed-valent compounds · nickel

[1] a) *Extended Linear Chain Compounds*, *Vol. 1–3* (Ed.: J. S. Miller), Plenum, New York, **1982**; b) S. Roth in *One-Dimensional Metals*, VCH, New York, **1995**; c) M. H. Chisholm, N. J. Patmore, *Acc. Chem. Res.* **2007**, *40*, 19 – 27; d) L. A. Barrios, D. Aguilà, O. Roubeau, P. Gamez, J. Ribas-Ariño, S. J. Teat, G. Aromí, *Chem. Eur. J.* **2009**, *15*, 11235 – 11243; e) J. K. Bera, K. R. Dunbar, *Angew. Chem.* **2002**, *114*, 4633 – 4637; *Angew. Chem. Int. Ed.* **2002**, *41*, 4453 – 4457; f) T. Rüffer, M. Ohashi, A. Shima, H. Mizomoto, Y. Kaneda, K. Mashima, *J. Am. Chem. Soc.* **2004**, *126*, 12244 – 12245; g) Y. Tatsumi, T. Murahashi, M. Okada, S. Ogoshi, H. Kurosawa, *Chem. Commun.* **2008**, 477 – 479; h) Y. Takemura, H. Takenaka, T. Nakajima, T. Tanase, *Angew. Chem.* **2009**, *121*, 2191 – 2195; *Angew. Chem. Int. Ed.* **2009**, *48*, 2157 – 2161.

[2] a) J. F. Berry, F. A. Cotton, L. M. Daniels, C. A. Murillo, *J. Am. Chem. Soc.* **2002**, *124*, 3212 – 3213; b) J. F. Berry, F. A. Cotton, C. A. Murillo, *Organometallics* **2004**, *23*, 2503 – 2506; c) J. F. Berry, F. A. Cotton, P. Lei, T. Lu, C. A. Murillo, *Inorg. Chem.* **2003**, *42*, 3534 – 3539; d) S.-Y. Lin, I-W. P. Chen, C.-h. Chen, M.-H. Hsieh, C.-Y. Yeh, T.-W. Lin, Y.-H. Chen, S.-M. Peng, *J. Phys. Chem. B* **2004**, *108*, 959 – 964; e) I-W. P. Chen, M.-D. Fu, W.-H. Tseng, J.-Y. Yu, S.-H. Wu, C.-J. Ku, C.-h. Chen, S.-M. Peng, *Angew. Chem.* **2006**, *118*, 5946 – 5950; *Angew. Chem. Int. Ed.* **2006**, *45*, 5814 – 5818; f) D.-H. Chae, J. F. Berry, S. Jung, F. A. Cotton, C. A. Murillo, Z. Yao, *Nano Lett.* **2006**, *6*, 165 – 168; g) K.-N. Shih, M.-J. Huang, H.-C. Liu, M.-D. Fu, C.-K. Kuo, G.-C. Huang, G.-H. Lee, C.-h. Chen, S.-M. Peng, *Chem. Commun.* **2010**, *46*, 1338 – 1340.

[3] a) J. F. Berry in *Multiple Bonds Between Metal Atoms* (Eds.: F. A. Cotton, C. A. Murillo, R. A. Walton), Springer, New York, **2005**, pp. 669 – 706; b) J. F. Berry, *Struct. Bonding (Berlin)* **2010**, *136*, 1 – 28; c) C.-Y. Yeh, C.-C. Wang, Y.-H. Chen, S.-M. Peng in *Redox Systems Under Nano-Space Control*, (Ed.: T, Hirao), Springer, Heidelberg, **2006**, pp. 85 – 115; d) C. Yin, G.-C. Huang, C.-K. Kuo, M.-D. Fu, H.-C. Liu, K.-N. Shih, Y.-L. Huang, G.-H. Lee, C.-Y. Yeh, C.-h. Chen, S.-M. Peng, *J. Am. Chem. Soc.* **2008**, *130*, 10090 – 10092.

[4] S.-M. Peng, C.-C. Wang, Y.-L Jang, Y.-H. Chen, F.-Y. Li, C.-Y. Mou, M.-K. Leung, *J. Magn. Magn. Mater.* **2000**, *209*, 80 – 83.

[5] a) D. Gatteschi, C. Mealli, L. Sacconi, *J. Am. Chem. Soc.* **1973**, *95*, 2736 – 2738; b) L. Sacconi, C. Mealli, D. Gatteschi, *Inorg. Chem.* **1974**, *13*, 1985 – 1991; c) A. Bencini, D. Gatteschi, L. Sacconi, *Inorg. Chem.* **1978**, *17*, 2670 – 2672; d) A. Bencini, E. Berti, A. Caneschi, D. Gatteschi, E. Giannassi, I. Invernizzi, *Chem. Eur. J.* **2002**, *8*, 3660 – 3670.

[6] a) I. P.-C. Liu, W.-Z. Wang, S.-M. Peng, *Chem. Commun.* **2009**, 4323 – 4331; b) I. P.-C. Liu, C.-F. Chen, S.-A. Hua, C.-H. Chen, H.-T. Wang, G.-H. Lee, S.-M. Peng, *Dalton Trans.* **2009**, 3571 – 3573; c) S.-A. Hua, I. P.-C. Liu, H. Hasanov, G.-C. Huang, R. H. Ismayilov, C.-L. Chiu, C.-Y. Yeh, G.-H. Lee, S.-M. Peng, *Dalton Trans.* **2010**, *39*, 3890 – 3896; d) S.-A. Hua, G.-C. Huang, I. P.-C. Liu, J.-H. Kuo, C.-H. Jiang, C.-L. Chiu, C.-Y. Yeh, G.-H. Lee, S.-M. Peng, *Chem. Commun.* **2010**, *46*, 5018 – 5020.

[7] a) K. Otsubo, A. Kobayashi, H. Kitagawa, M. Hedo, Y. Uwatoko, H. Sagayama, Y. Wakabayashi, H. Sawa, *J. Am. Chem. Soc.* **2006**, *128*, 8140 – 8141; b) M. Yamashita, S. Takaishi, A. Kobayashi, H. Kitagawa, H. Matsuzaki, H. Okamoto, *Coord. Chem. Rev.* **2006**, *250*, 2335 – 2346; c) K. Uemura, K. Fukui, Hi. Nishikawa, S. Arai, K. Matsumoto, H. Oshio, *Angew. Chem.* **2005**, *117*, 5595 – 5600; *Angew. Chem. Int. Ed.* **2005**, *44*, 5459 – 5464; d) M. Mitsumi, H. Ueda, K. Furukawa, Y. Ozawa, K. Toriumi, M. Kurmoo, *J. Am. Chem. Soc.* **2008**, *130*, 14102 – 14104.

[8] I. P.-C. Liu, M. Bénard, H. Hasanov, I-W. P. Chen, W.-H. Tseng, M.-D. Fu, M.-M. Rohmer, C.-h. Chen, G.-H. Lee, S.-M. Peng, *Chem. Eur. J.* **2007**, *13*, 8667 – 8677.

[9] a) M. B. Robin, P. Day, *Adv. Inorg. Chem. Radiochem.* **1968**, *10*, 247 – 422; b) M. D. Ward, *Chem. Soc. Rev.* **1995**, *24*, 121 – 134; c) B. S. Brunschwing, C. Creuts, N. Sutin, *Chem. Soc. Rev.* **2002**, *31*, 168 – 184; d) K. D. Demadis, C. M. Hartshom, T. J. Meyer, *Chem. Rev.* **2001**, *101*, 2655 – 2686.

[10] a) N. S. Hush, *Coord. Chem. Rev.* **1985**, *64*, 135 – 157; b) N. S. Hush, *Prog. Inorg. Chem.* **1967**, *8*, 391 – 393; c) F. A. Cotton, C. Y. Liu, C. A. Murillo, D. Villagran, X. Wang, *J. Am. Chem. Soc.* **2003**, *125*, 13564 – 13575.

[11] P. Kiehl, M.-M. Rohmer, M. Bénard, *Inorg. Chem.* **2004**, *43*, 3151 – 3158.

[12] a) J. J. Borrás-Almenar, J. M. Clemente-Juan, E. Coronado, B. S. Tsukerblat, *Inorg. Chem.* **1999**, *38*, 6081 – 6088; b) J. J. Borrás-Almenar, J. M. Clemente-Juan, E. Coronado, B. S. Tsukerblat, *J. Comput. Chem.* **2001**, *22*, 985 – 991.

